HELIOS

Highly rEliable LInks during sOlar conjunctionS

Executive Summary

ITT Reference: AO/1-8050/14/F/MOS
Reliable TT&C during Superior Solar Conjunctions

Partners:

Radio Science and Planetary Exploration Laboratory
University of Bologna
Headquarters: Via Fontanelle 40, 47121 Forlì (FC) - Italy
Phone: +39 0543374456 fax: +39 0543374477 E-mail: paolo.tortora@unibo.it
Web: http://www.radioscience.unibo.it

TABLE OF CONTENTS - Acronyms

DOCUMENT SIGNATURE TABLE			
	Name	**Function**	**Signature**
PREPARED BY	Paolo Tortora	Study Manager	
	Aurel Zeqaj	Project Engineer	
	Enrico Paolini	Project Engineer	
	Andrea Giorgetti	Project Engineer	
	Alan Stocker	Leicester Team Coordinator	
	Dave Siddle	Project Engineer	
	Mike Warrington	Project Engineer	
	Antonios Argyriou	Thessaly Team Coordinator	
	Thanasis Korakis	Project Engineer	
	Leandros Tassiulas	Project Engineer	
REVIEWED BY	Aurel Zeqaj	Project Engineer	
APPROVED BY	Paolo Tortora	Study Manager	

DOCUMENT CHANGE RECORD			
ISSUE/REVISION	**DATE**	**DELIVERABLE CODE**	**LIST OF CHANGES**
1.0	26/04/2018	D11	First Issue
1.1	02/05/2018	D11	Revised document after Teleconf with ESA

TABLE OF CONTENTS

LIST OF FIGURES

LIST OF TABLES

1 INTRODUCTION

This Technical Documentation has been prepared in response to ESA's AO/1-8050/14/F/MOS, entitled:

Reliable TT&C during Superior Solar Conjunctions

and is fully compliant with the technical requirements of the ITT.

The HELIOS project has investigated the effect of the solar corona on the performance of spacecraft communications (both TC and TM) during superior solar conjunctions. Highlights include the development of:

- a channel model that allows (for X-band) accurate simulation of amplitude and phase effects at SEP angles as low as 1° (it can also be scaled to Ka and S-band);
- a simulator that allows the testing of a wide range of modulation and coding methods;
- an analytic model to predict the performance of a PLL under fading conditions.

These tools enabled us to draw the following conclusions

- that for X-band TC and TM will be able to operate using coherent modulation methods at SEP>2° (albeit at lower data rates than in free space);
- for Ka-band, TC and TM will be possible with coherent modulation methods at SEP~1°
- for X-band, non-coherent modulation (e.g. FSK) is possible at SEP>1° (again, with relatively low data rates), but should not be used to replace coherent methods where these are possible.

1.1 Acronyms

Abbreviation	Meaning
AD	Applicable Document
BER	Bit Error Rate
BPSK	Binary Phase-Shift Keying
CCSDS	Consultative Committee for Space Data Systems
DSN	Deep Space Network
ECSS	European Cooperation for Space Standardization
ESA	European Space Agency
FER	Frame Error Rate
FSK	Frequency-Shift Keying
GMSK	Gaussian Minimum-Shift Keying
GUI	Graphical User Interface
IFMS	Intermediate Frequency and Modem System
LDPC	Low-Density Parity Check
LoS	Line of Sight
NASA	National Aeronautics and Space Administration
PLL	Phase-Locked Loop
PSD	Power Spectral Density
PSK	Phase-Shift Keying

Abbreviation	Meaning
QPSK	Quadrature Phase Shift Keying
RD	Reference Document
S/C	Spacecraft
S/W	Software
SEP	Sun-Earth-Probe angle
SoW	Statement of Work
SPE	Sun-Probe-Earth angle
TT&C	Telemetry, Tracking & Command
USO	Ultra-Stable Oscillator

Table 1-1 Acronyms

2 APPLICABLE AND REFERENCE DOCUMENTS

2.1 Applicable Documents

Ref.	Title
[AD. 1]	CCSDS 131.0-B-2, TM Synchronization and Channel Coding. Blue Book. Issue 2. August 2011.
[AD. 2]	CCSDS 414.1-B-1, Pseudo-Noise (PN) Ranging Systems. Issue 1. March 2009.
[AD. 3]	IFMS Users' manual /BAE Systems
[AD. 4]	Technical Note "Technical Note 2: Architectural Report" Version 1.5 for ITT AO/1-8050/14/F/MOS, HELIOS: Highly rEliable LInks during sOlar conjunctionS
[AD. 5]	Technical Note "Technical Note 3A: Analysis of Current Architecture and Methods" Version 1.5 for ITT AO/1-8050/14/F/MOS, HELIOS: Highly rEliable LInks during sOlar conjunctionS
[AD. 6]	Technical Note "Thechnical Note 4 : Improved architecture and methods for reliable solar conjunction links" Version 1.5 for ITT AO/1-8050/14/F/MOS, HELIOS: Highly rEliable LInks during sOlar conjunctionS
[AD. 7]	810-005, Rev E, DSMS Telecommunications link design handbook, 207, Rev. A, 34-m and 70-m Telemetry reception.
[AD. 8]	CCSDS, "SHORT BLOCK LENGTH LDPC CODES FOR TC SYNCHRONIZATION AND CHANNEL CODING ", Apr. 2015, ORANGE BOOK, 230.1-G-X

Table 2-1 Applicable Documents

2.2 Reference Documents

Ref.	Title
[RD. 1]	Reliable TT&C during Superior Solar Conjunctions – Support Technical Note. ESA/ESOC GSRT-STU-MEM-1001-HSO-GSY
[RD. 2]	David Morabito and Rolf Hastrup "Communicating with Mars During Periods of Solar Conjunction", IEEE Aerospace Conference Proceedings, 2002.

Ref.	Title
[RD. 3]	CCSDS, Tm synchronization and channel coding summary of concept and rationale, CCSDS 130.1-G-2

3 Introduction

During a deep space mission, the TT&C link between the spacecraft and the Ground Station, can be severely degraded if a superior solar conjunction, i.e. when the spacecraft is located behind the Sun with respect to the Earth, occurs.

This is due to the fact that as the Sun-Earth-Probe (SEP) angle reduces, there is an increased degradation in terms of amplitude and phase scintillation, and spectral broadening, which is caused by electron density inhomogeneities, and by the solar wind that moves the plasma blobs in the medium across the carrier wave path. Depending on the size of the inhomogeneities (or "blobs") in the plasma, they can effect or not the amplitude scintillation, due to Fresnel filtering (Figure 3-1).

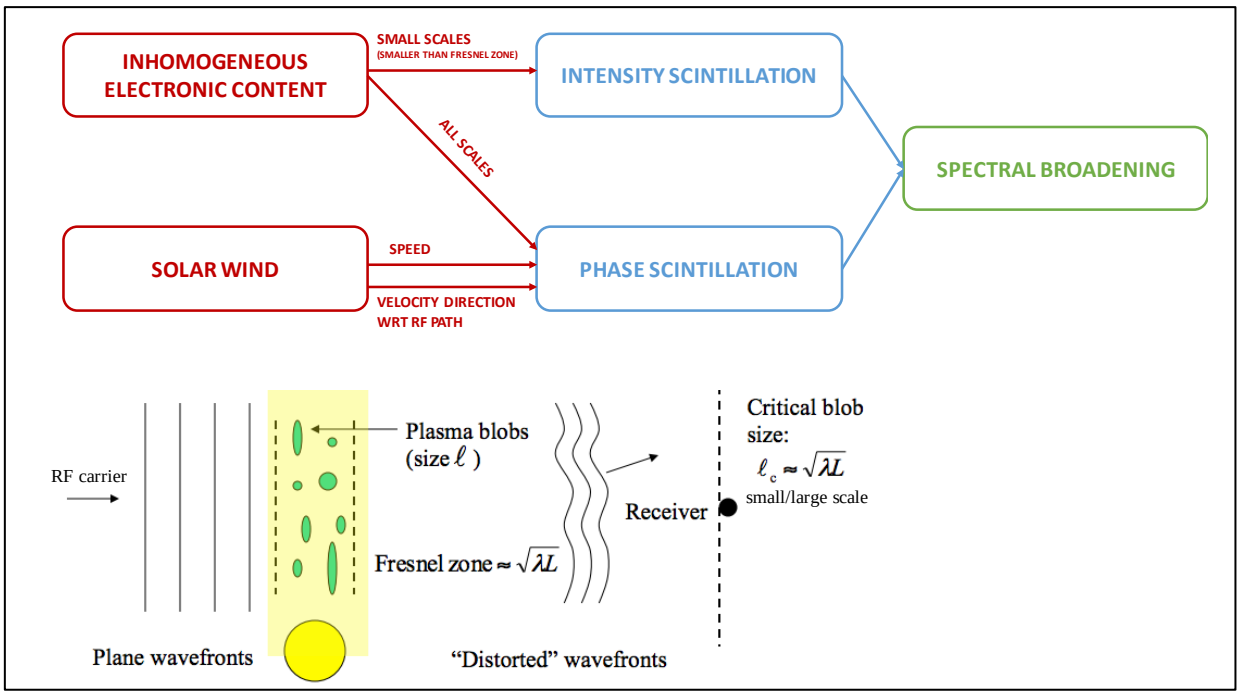

Figure 3-1 - Solar plasma effects on RF signals.

4 Objective of the study

The purpose of this study is the definition of a communication subsystem architecture (including both ground and space segments, as well as operational methods) that allows robust RF TT&C links during superior solar conjunction phases. The defined architecture shall ensure robust and reliable links in scintillation regimes (i.e. at low SEP angles) where TT&C links are nowadays degraded, leading to occasional link interruptions. Similarly, the defined architecture shall ensure that at even higher scintillation regimes (i.e. very low SEP angles, where scintillations still dominate over thermal noise effects due to pointing to the sun), TT&C links can be established (these links are not possible today). The objective is thus to ensure reliable links (to cover any potential TT&C need), rather than to maximize data volumes.

5 Channel model

An empirically derived channel model that works at X-band and can be scaled to Ka-band was developed. This was derived analysing the open loop data of Mars Express, during a superior solar conjunction in 2013 and then comparing the values of the amplitude scintillation, phase scintillation, and spectral broadening with the relevant models and observations previously reported in literature.

The channel model for a one-way link between two participants, is broadly defined as:

$$h(t) = A(t)e^{j\theta(t)} \qquad 5\text{-}1$$

Where $A(t)$ is the amplitude term and $\theta(t)$ is the channel phase term both including the scintillation that we want to model.

The amplitude $A(t)$ has been described modeling the PSD of the observed amplitude with a Gauss-Markov process, found by fitting observed data.

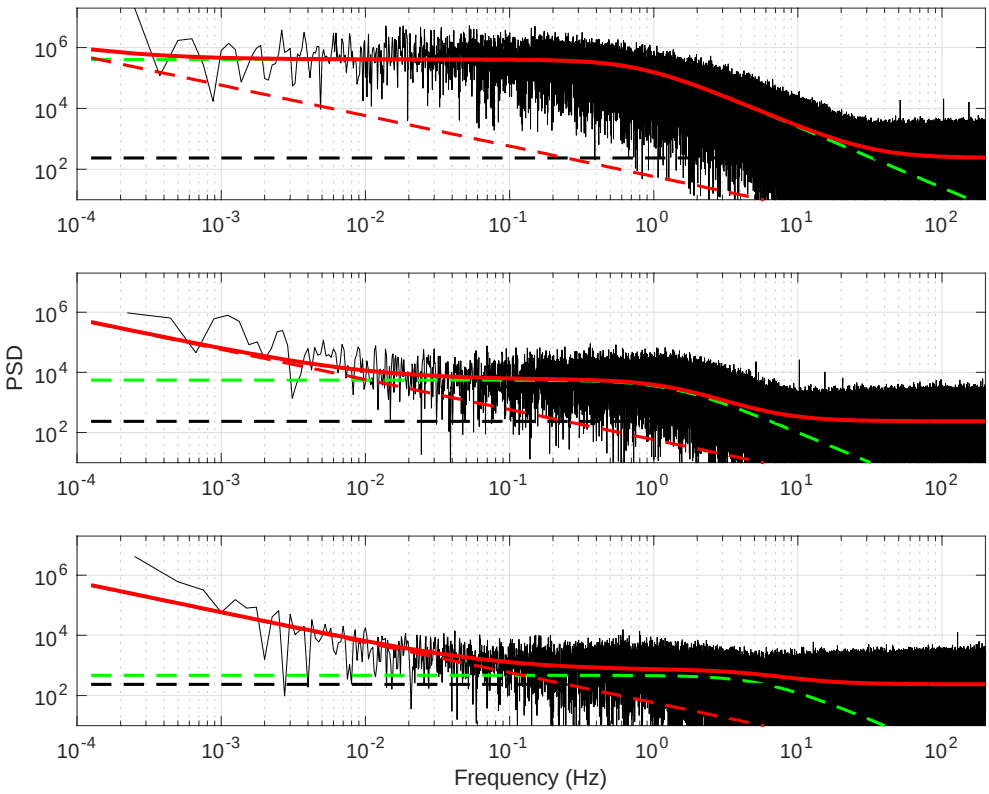

Figure 5-1 : PSD spectrum of amplitude scintillation for (from the top) SEP=2.4°, 5.6°, and 9.0°. The best-fit curves of the overall PSD (solid red line), the white noise floor (dashed black line), solar effects (dashed green line), and pink noise (dashed red line) are also indicated.

An example PSD spectrum of the amplitude scintillation is presented in Figure 5-1. Three parts to the spectrum have been identified.

- A white noise component that is observed at frequencies higher than about 10 Hz in the two higher SEP examples (this frequency tends to get higher when the SEP is lower). The PSD level associated with this region is independent of SEP except for SEP<1.5° and corresponds to the thermal noise.

- A second 'white noise' region where the PSD is flat as a function of frequency that corresponds to the scintillation introduced by the solar corona. For SEP=5.6°, this lies between 0.01 and 1 Hz, with a transition region between this and the white noise at higher frequencies (i.e. between 1 and 10 Hz). The PSD level of this region is strongly dependent on SEP.

- A pink noise component at lower frequencies and more noticeable at higher values of SEP (e.g. 5.6° and 9.0°). In the example for SEP=9.0°, this is observed at frequencies below about 0.01 Hz. The PSD level of the pink noise does not appear to systematically depend on SEP, although there is some variation from pass to pass.

The phase, θ(t) has been described by modelling the PSD of the observed phase with a straight line, found by fitting observed data. An example phase PSD is presented in Figure 5-2.

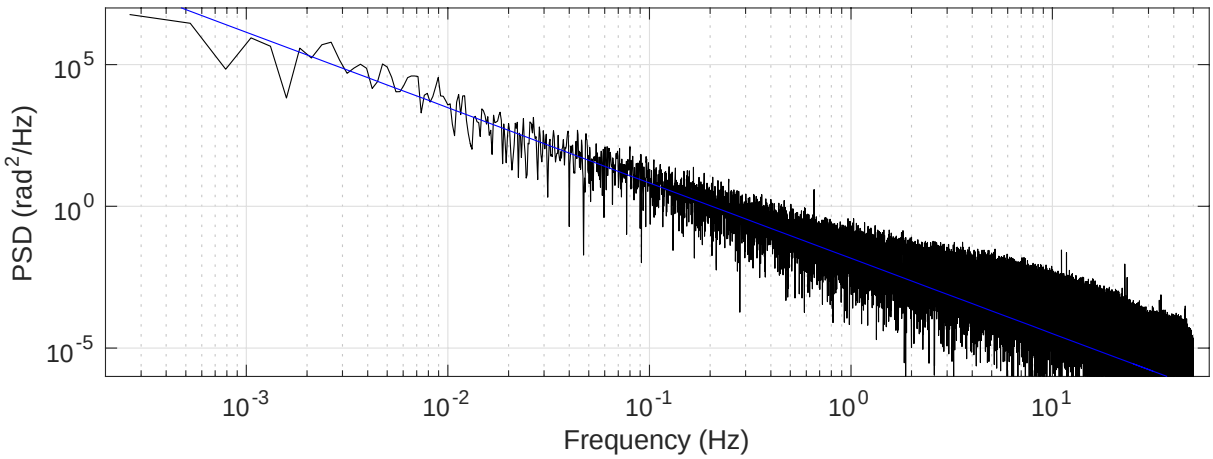

Figure 5-2 : The power spectral density of the phase for an X-band signal on 9 April 2013 for 0737–0840 UT. The straight line is the least-squares fit evaluated between 2x10^{-3} and 0.1 Hz (the gradient is -2.66 and the value at 1 Hz is 10$^{-1.83}$).

For both the amplitude and the phase, the values derived from the PSD spectra have been found as a function of SEP. In synthesising the channel in-phase and quadrature values, the amplitude and phase components have been combined using Equation 5-1.

6 Coherent Demodulation

Depending on the type of link, bit (and frame) errors can occur due to failure to track changes in the phase (whether a result of the solar plasma or thermal noise), or amplitude fading. In this respect, the PLL bandwidth ($2B_L$) is fundamental, since a correct definition can give the threshold between a correct or incorrect carrier tracking. For this reason, we introduced a model (here known as an 'analytic' model, although it is actually a semi-empirical model) for the phase variance that will allow the PLL parameters required for optimum performance to be determined.

6.1 Basic model (without fading)

The total variance, σ_φ^2 is the sum of the phase variance due to the solar coronal scintillation, σ_S^2 and that due to thermal noise, σ_N^2. The thermal noise in the PLL is simply proportional to the two-sided PLL bandwidth, $2B_L$, but the solar variance is a more complicated function of the SEP angle in degrees and $2B_L$ in Hz. This can be expressed as:

$$\sigma_\varphi^2 = \frac{C_{band} C_{pll} C_q}{\beta^q (2B_L)^r} + \frac{2B_L}{2\,SN0_{PLL}} \qquad 6\text{-}1$$

where β is simply the SEP angle in degrees for X-band, but a function of β for S- and Ka-band; C_{band} depends on whether S, X or Ka band is used and on whether the link is an uplink, downlink or an up and down link; C_{pll} depends on whether the PLL used is critically damped or underdamped and C_q depends on the signal quality. The signal quality may be chosen to be 'good', 'moderate' or 'poor' and will determine whether the values in the model are derived from the lower decile, median or upper decile of the scintillation distribution in the data. Furthermore, the exponents, *q* and *r* as well as C_{band}, C_{pll} and C_q take on different values for β<4.7 and β>4.7.

The values of the constants and exponents are given in the project's final report [AD10], but an example here for clarification. A downlink using a critically damped PLL at X-band in with SEP = 2° and an assumption of poor signal quality will give β = 2; q = 4.402; r = 1.698; C_{band} = 2.1271; C_{pll} = 1.000 and C_q = 12.963, giving:

$$\sigma_\varphi^2 = \frac{2.1271 * 1 * 12.963}{2^{4.402}(2B_L)^{1.698}} + \frac{2B_L}{2\,SN0_{PLL}} = \frac{1.3042}{(2B_L)^{1.698}} + \frac{2B_L}{2\,SN0_{PLL}} \qquad 6\text{-}2$$

Differentiating 6-1 and equating it to zero gives the following expression for the optimum value of $2B_L$ (i.e. the value that gives the minimum σ_φ^2):

$$(2B_L)_{opt} = \left[\frac{2\,SN0_{PLL} C_{band} C_{pll} C_q r}{\beta^q}\right]^{\frac{1}{r+1}} \qquad 6\text{-}3$$

The PLL bandwidth, 2BL, should be chosen such that it is (see Figure 6-1):

1. large enough to minimise the phase variance caused by the solar plasma;
2. small enough to minimise the thermal noise contribution from the PLL;
3. small enough to maintain an adequate SNR such that the effect of thermal phase jumps (see previous section) is minimised (SNR>10 dB). If there is insufficient carrier power to obtain the required SNR, then increasing 2BL (at the expense of a further reduction in SNR) or decreasing the sample rate will minimise the effect of the phase jumps.

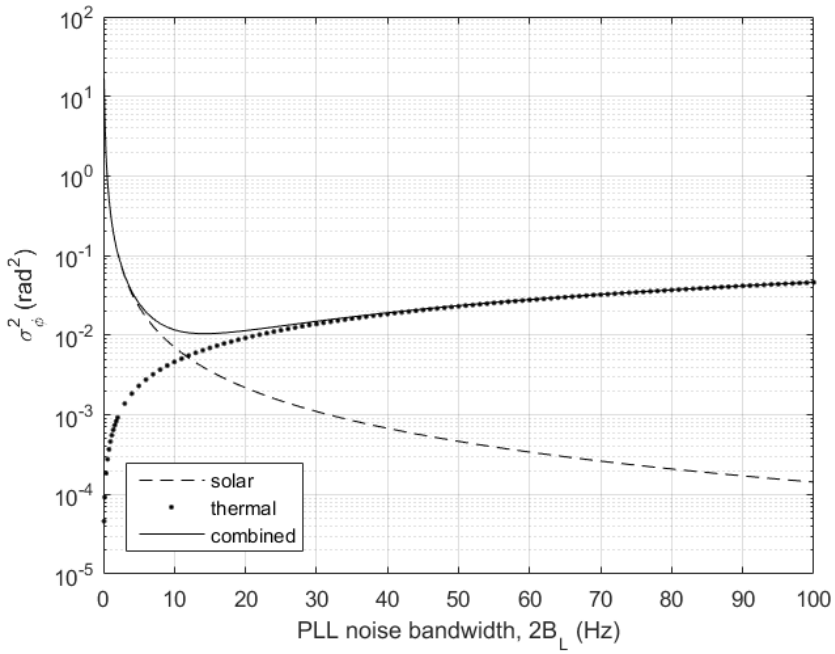

Figure 6-1 : Phase noise vs PLL Bandwidth (2BL) derived from analytical model for the Jupiter TC Scenario (see Section 7).

6.2 Fading model

The model introduced in Section 6.1neglects the amplitude fading so is limited to SEP angles for which this is relatively small (e.g. for X-band, at SEP=3°, the fading depth~3 dB). The fading model described below determines the phase variance that is exceeded *p*% of the time, based on the amplitude probability density distributions from thirty-two observed Mars Express 2013 data files. Each file was fitted to a Nakagami distribution, which is defined for positive values of *x* (here representing the received signal amplitude) using parameters μ (>1/2) and ω (> 0) by:

$$N(x,\mu,\omega) = \frac{2\mu^{\mu}x^{(2\mu-1)}}{\omega\Gamma(\mu)} exp\left(\frac{-\mu x^2}{\omega}\right) \qquad 6\text{-}4$$

Once omega and mu have been parametrised, a distribution of amplitude for any SEP angle and any percentile can be found from these parameters. For low SEP, the Nakagami distribution was a better fit to the observations than the Rician distribution often employed.

The probability, $P_{critical}$, that the PLL will have difficulty in tracking the phase is presented in a form in Figure 6-2 and

Figure 6-3 that allows the impact of different values of CN0 and 2BL on performance to be assessed. In the following discussion, we have followed the recommendation that for a residual carrier, the PLL be operated such that the phase variance is less than a threshold of 0.1 rad^2. When the phase variance exceeds this threshold, it is more likely that the PLL will not successfully track the phase. If only thermal noise is present (i.e. the effect of the solar plasma is small, e.g. when SEP is large) then this condition will occur when the double-sided in-loop SNR is less than approximately 7 dB. For an X-band downlink at SEP = 1, CN0 would have to exceed 40 dB Hz by a significant margin before $P_{critical}$ is reduced sufficiently for reliable PLL operation (even at 50 dB Hz, which is close to the maximum expected in current missions $P_{critical}$ remains too high). For Ka-band, the situation is much better and the PLL should be able to operate reliably with achievable values of CN0.

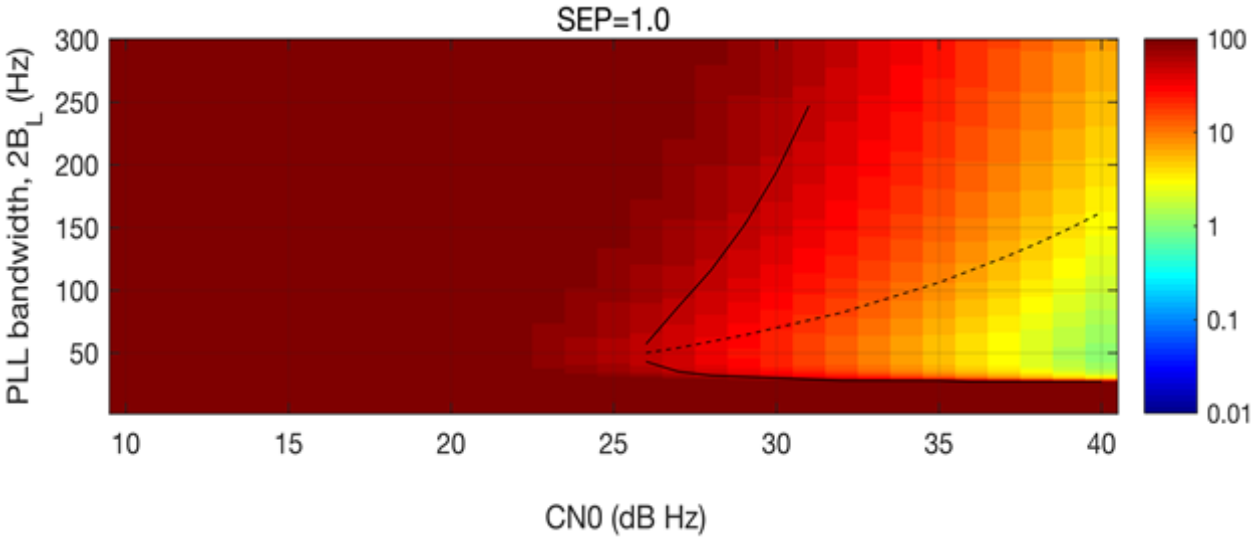

Figure 6-2 : $P_{critical}$ (%) (i.e. where phase variance>0.1 rad^2) as a function of PLL bandwidth and CN0 for an X-band downlink at SEP of 1.0°. The solid black lines represent the minimum and maximum values of 2BL for which σ^2_{loop}<0.1 rad^2 (neglecting fading), while the dashed line (either black or white for clarity) represents the optimum 2BL (i.e. where the phase variance is minimised, neglecting fading)

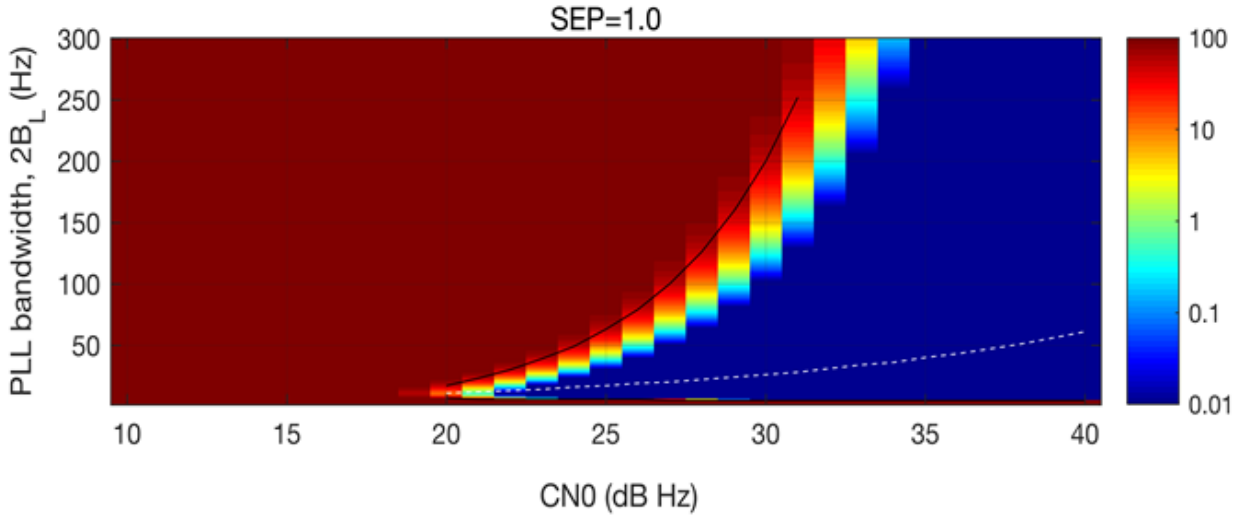

Figure 6-3 : As for Figure 6-2, except for Ka-band downlink

Similar results obtained for operation of the PLL with BPSK modulation can found for GMSK modulation. The difference here, is that since there is no longer a decoupling between data and carrier, the squaring loss should be taken into account and moreover the phase variance limit for which the PLL is less likely to operation correct is reduced from 0.1 rad^2, to 0.005 rad^2 (Section 5.3.3 in [AD. 7]).

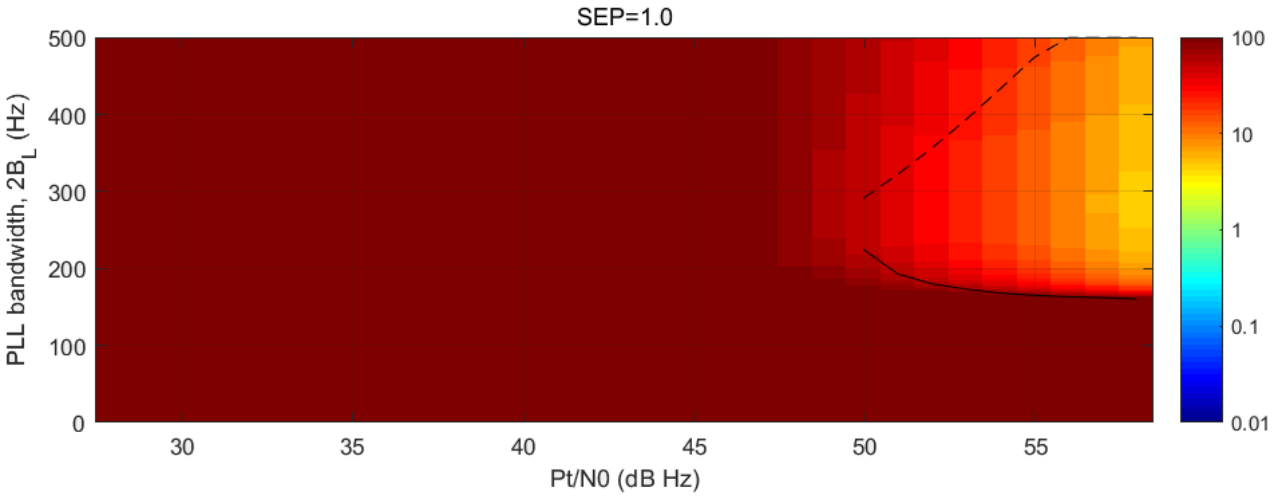

Figure 6-4 : $P_{critical}$ (%) (i.e. where phase variance>0.005 rad^2) as a function of PLL bandwidth and Pt/N0 for an X-band downlink at SEP of (from top to bottom) 1.0 and 3°, with a symbol rate of 62.5 ksps. The solid black lines represent the minimum and maximum values of 2BL for which the total phase variance<0.005 rad^2 (neglecting fading), while the dashed line (either black or white for clarity) represents the optimum 2BL (i.e. where the phase variance is minimised, neglecting fading)

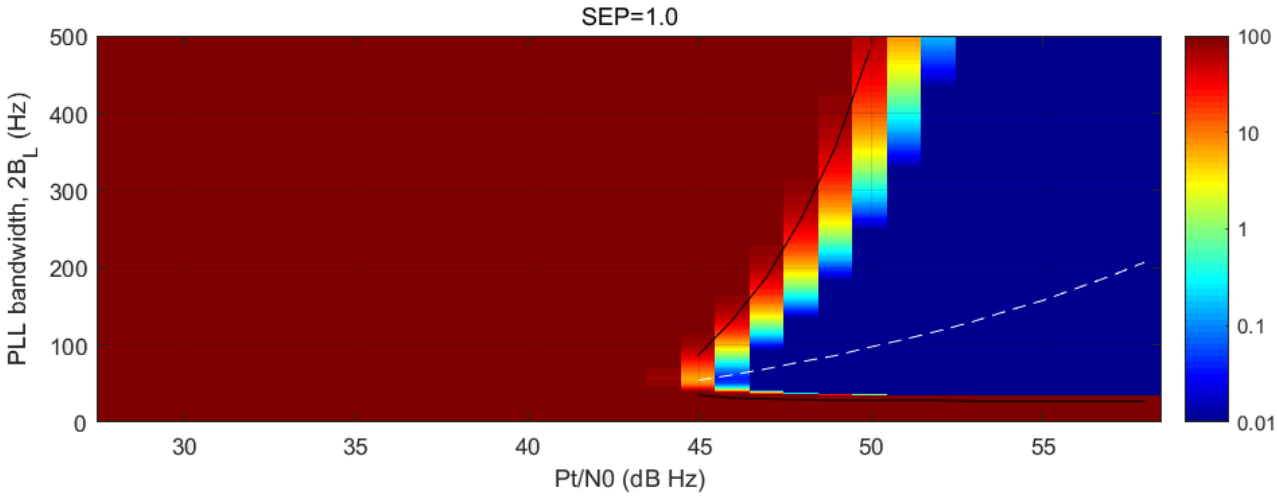

Figure 6-5 : As for Figure 6-4 but for Ka-band

7 Analysis of current communication subsystems architecture and operational methods

Using the models and simulator developed as part of this project, the existing communication subsystem architecture and operational methods have been analysed in order to identify the critical points. This analysis has been performed for the complete link (i.e. end to end), using the current modulation, i.e. BPSK, and coding schemes, i.e. BCH in TC and Turbo 1/4 for TM. This analysis was aimed at enabling improvements to the existing communication subsystem architecture (for both ground and space segment), as well as tailoring operational procedures. The analysis has been undertaken for X-band and at an SEP=3°. The effects of amplitude fading have been neglected in the analysis reported

below, but since the fading depth is 3 dB for X-band at 3°, this will have a relatively small effect (e.g. in the limit, the simulated data rates will need to be halved). The analysis process was performed on some contingency scenarios (see Section 7 of [AD. 5]), in order to evaluate the link performances and to show that the use of an optimum PLL Bandwidth value can provide a more reliable link. As an example, an hypothetical scenario at Jupiter is used (see Table 7-1 for the details). The simulation process consist in examining at first the nominal setup, and then trying to optimize it by choosing the optimum PLL Bw for that particular scintillation regime. This operation is done using equation 6-3 (see Figure 6-1) and then verified against the simulator. In this particular case, the optimum PLL double-sided bandwidth (2BL) is about 12 Hz.

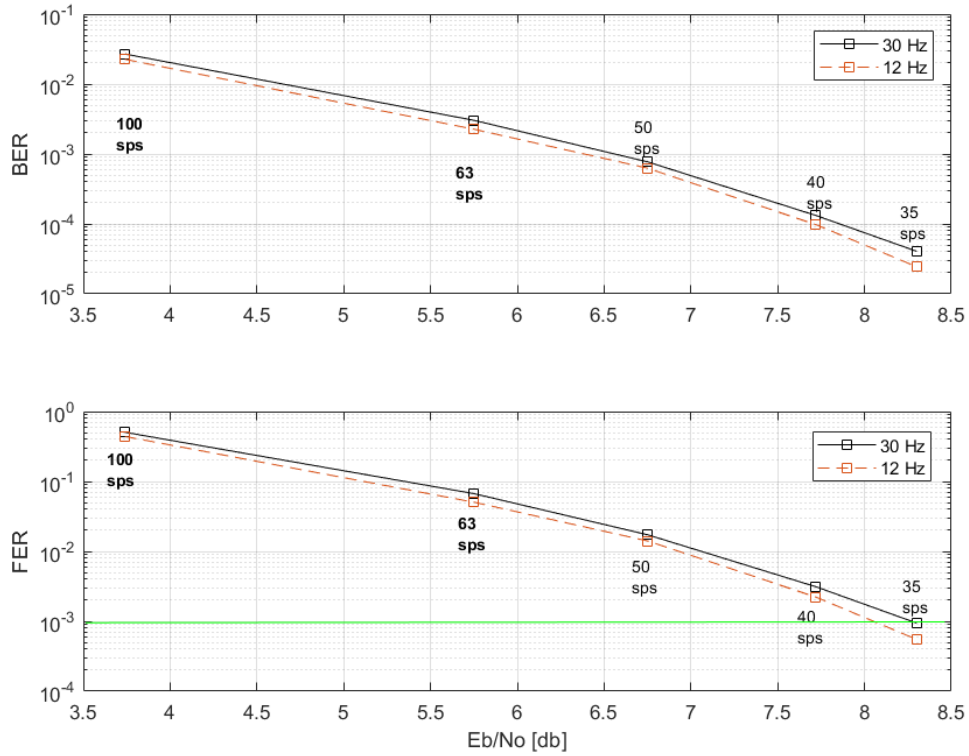

Figure 7-1: Bit Error Rate (BER) and Frame Error Rate (FER) vs Eb/No for two different PLL Bandwidth (10, 30 Hz) for the Jupiter TC Scenario.

Jupiter TC	Nominal configuration	Optimized configuration
S/N0 [dB Hz]	31.15	-
Modulation index (m) [rad]	0.6	-
Coding scheme	BCH	-
$2*B_L$ [Hz]	30	12
SNR_{PLL} [dBHz]	19.2	15.6
B_s [sps]	8	16

Table 7-1 : Nominal and optimized configuration for Jupiter TC Scenario (SEP = 3)

Once the optimum PLL Bw has been determined, the maximum symbol rate that permits to have a feasible link, i.e. a FER = 10^{-3} for the TC case and a FER = 10^{-5} for TM can be found. This process is done by decreasing the symbol rate progressively (and so increasing the Eb/N0) until the desired performance level is reached. An example can be seen in Figure 7-1. So, what we could conclude was that the link was surely feasible (and not only for this case, but for all the contingency Scenarios provided) with the configuration provided by the Agency (the BER/FER are significantly higher than the target values, i.e. $10^{-3}/10^{-5}$). But there is still some space to optimize even further the operational configuration. In fact, the usage of the optimum PLL bandwidth, i.e. the one that minimizes the phase variance, gives the opportunity to improve the performance. As said previously, fading was neglected for the simulations of this Section– a straightforward solution is to add 3 dB (the X-band fading level at SEP=3) to the required EbN0 to provide fading margin, if this is feasible, or to reduce the data rate by a factor of a half.

8 Proposed and Tested Alternatve Solutions

Going to lower SEP values, the operability of the PLL at X-band becomes lower and lower, till for an angle equal to 1°, there is the need to find alternative solutions, as can be seen in Figure 6-2[1]. For this reason ,there is the need to find some alternative solution to make a feasible link also at very low SEP angles. This can be achieved using non-coherent MFSK or, potentially, some diversity techniques, i.e. frequency or spatial. Changing frequency band from X-band to Ka-band will improve the robustness of TC/TM links since, for Ka-band, the performance at SEP=1° is approximately the same as the performance at SEP = 3° for X-band. For SEP angles where the PLL is likely to remain operational the benefits of using a new coding scheme, i.e. LDPC for TC/TM is also explored.

8.1 New coding schemes

For the TC case[2], the use of Low Density Parity Check (LDPC) codes is already a viable option, since the 64/128 and 256/512 LDPC have already been included in the standard [AD. 8]. What we confirmed with our simulations is that this two codes are an alternative to the standard BCH (57/63) code. Taking a look at Table 8-1, it is immediately clear how as the SEP angle decreases, i.e. down to 2° (since this is an SEP angle where the PLL is able to operate with achievable CN0), the two short LDPC codes get a better gain (in dB) with respect to the standard BCH (besides having also better performances) to achieve the operable FER, i.e. 10^{-3}.

SEP (deg)	Standard BCH 57/63	Delta-Eb/N0 for LDPC 64/128	Delta-Eb/N0 for LDPC 256/512
2	9.8 dB	+5.1 dB	+6.2 dB
3	8 dB	+3.6 dB	+4.9 dB
4	7.8 dB	+3.5 dB	+4.7 dB
AWGN	7.65 dB	+3.35 dB	+4.35 dB

Table 8-1 : Minimum value of Eb/N0 required for the BCH code to reach FER = 10^{-3} at different SEP, and gain (in dB) of the LDPC with respect to the BCH (positive values indicate better performance, i.e. same FER with lower Eb/N0).

[1] This obviously is the case for most of the contingency scenarios that were a subject of this study, but probably for some nominal cases, where the S/N0 and C/N0 are higher, the link may be feasible even with an X-band link. This seems to be more the case for a SEP = 1.5° than at 1°, given that for the latter even with a C/N0 = 50dBHz the link is still almost probably not feasible.
[2] The simulations for this Section did not properly account for amplitude fading, and the results appear to be different if this is included.

Moreover, it is really interesting to note how, if SNR_{PLL} is high enough, such that the phase variance is below a threshold of 0.1 rad^2, which for the AWGN case occurs at 7 dB, the performance of the link is not affected by the S/N0 (see Figure 8-1). Note that, in the case of Figure 8-1, the PLL Bw used is fixed, so as a consequence is not the optimum for each point. If this would have been the case, the isolines would have been vertical (till the minimum SNR_{PLL} value, i.e. 7 dBHz), meaning that the performances are independent of the S/N0 provided enough power is available for the carrier.

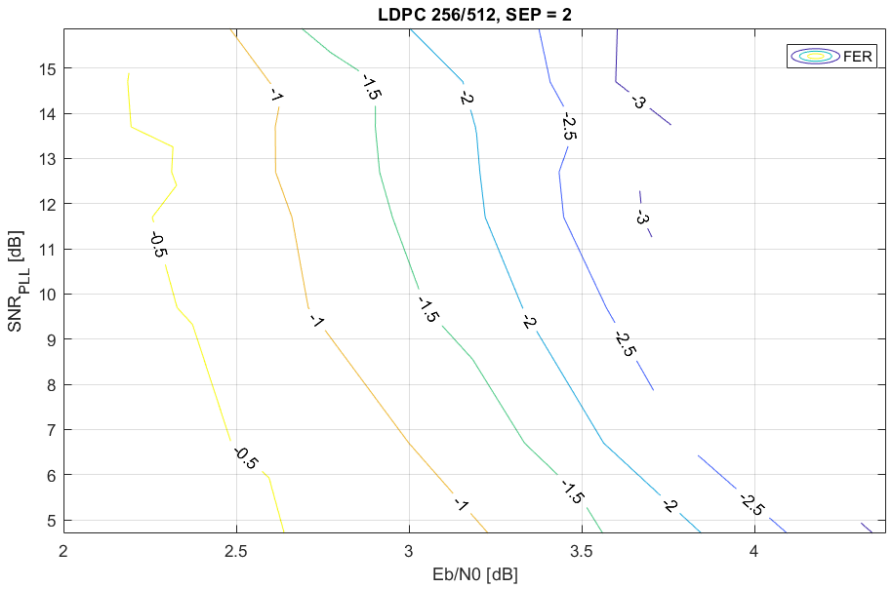

Figure 8-1 : Isolines of FER (Frame Error Rate) for different values of Eb/N0 and SNR_{PLL}.

For the TM case, as well, the LDPC [RD. 3] codes were considered . In particular, we tried to understand if they are a valid alternative to the standard Turbo codes.

SEP (Deg)	LDPC 1024	LDPC 4096	Turbo 1/2	Turbo 1/4	Turbo 1/6
2	~2.5 dB	~1.8 dB	1.55 dB	~0.3 dB	~-0.05 dB
3	~2.03 dB	~1.4 dB	~1.38 dB	0.24 dB	~-0.1 dB
4	~2.01 dB	~1.32 dB	~1.25 dB	~0.23 dB	-

Table 8-2 : minimum value of Eb/N0 [dB] required for the different codes to reach FER = 10^{-5} at different SEP[3]

Taking into consideration Table 8-2, and considering only the codes with code rate equal to 1/2 to have a fair comparison, is clear that the Turbo code has an advantage over the shorter LDPC code , i.e. k= 1024 both in terms of the minimum Eb/N0 [dB] and as a consequence also in terms of maximum bit rate. Moreover the Turbo code encoder is also less complex than the one of the LDPC codes. While with the respect to the "medium length" LDPC, i.e. k = 4096 the advantage is not so marked. The only drawback of the Turbo ½ code is the fact that after a certain Eb/N0 there is an "error floor", that in the case of SEP =2°,3° happens exactly at the target FER, i.e. 10^{-5}. So, as long as this is our target value, the Turbo code should have an advantage over the LDPC codes (even if, probably the LDPC k = 4096

[3] Most of the values in the table are extrapolated from the performance curves, since getting a FER = 10^{-5} required a simulation time too high to be performed

should be the safest choice since even a small change in the solar condition could bring to a failure of the Turbo code), while if one aims at lower FER values, then LDPC codes should be the choice[4].

8.2 Non-coherent FSK Modulation

Frequency-Shift Keying (FSK) is a form of digital modulation that represents digital data through discrete variations in the frequency of a carrier signal. In FSK, the instantaneous frequency (or tone) of a constant-amplitude carrier signal is changed between two (for BFSK) or more values (for M-ary FSK) by the baseband digital message signal m(t). This occurs at the beginning of each signal/symbol interval T, to represent symbol states. The carrier signal amplitude remains constant. In M-ary FSK, the minimum frequency spacing to maintain orthogonality between carriers is: $2\Delta f_{min} = R_S/2 = 1/(2T_S)$ for coherent detection, and $2\Delta f_{min} = R_S = 1/T_S$ for non-coherent detection.

In order to have an idea of the potentiality of the non-coherent modulation at low SEP angles, a set of simulation[5] was performed using an MFSK modulation, with different M values, i.e. 2, 4, 8, 16, at first without any coding, and then using an LDPC with different frame length for TC and TM. The results of the uncoded case were compared with those of the LDPC codes in order to see, first of all if the link was feasible at SEP = 1° for our contingency cases of interest and then also to see how the LDPC codes, that are in principal not designed for this kind of modulation, perform.

modulation	Eb/N0 to have BER = 10^{-5} [dB]	Gain with respect to 2-FSK [dB]
2-FSK	38	-
4-FSK	35	3
8-FSK	33.6	4.4
16-FSK	32.7	5.3

Table 8-3 : Values of Eb/N0 [dB] for which the target BER, i.e. 10^{-5} is reached at SEP = 1 ° for the Uncoded non-coherent M-FSK modulation at an S/N0 = 28 dBHz and the respective gains with respect to the non-coherent 2-FSK.

modulation	Eb/N0 to have FER = 10^{-3} [dB]	Gain with respect to 2-FSK [dB]
2-FSK	13.6	-
4-FSK	12.3	1.3
8-FSK	11.8	1.8
16-FSK	11.7	1.9

Table 8-4 : Values of Eb/N0 [dB] for which the target FER, i.e. 10^{-3} is reached at SEP = 1° for the LDPC k =256 non-coherent M-FSK modulation at an S/N0 = 28 dBHz and the respective gains with respect to the 2-FSK.

In conclusion, the link is feasible at SEP = 1 using an MFSK modulation for all the Contingency Scenarios provided, for both TC and TM, obviously at the cost of low symbol rates. Moreover by taking a look at Table 8-3 and Table 8-4, the 8-FSK modulation seems like the most promising case, since the gain between 16-FSK with respect to 8-FSK is very little to justify its use.

[4] Moreover, the longest LDPC code, i.e. k = 16384, that was not simulated, could provide a further advantage in terms of performances (most probably even better than the Turbo ½), and without any error floor.
[5] For the simulations of this Section, effect of amplitude fading is fully accounted for.

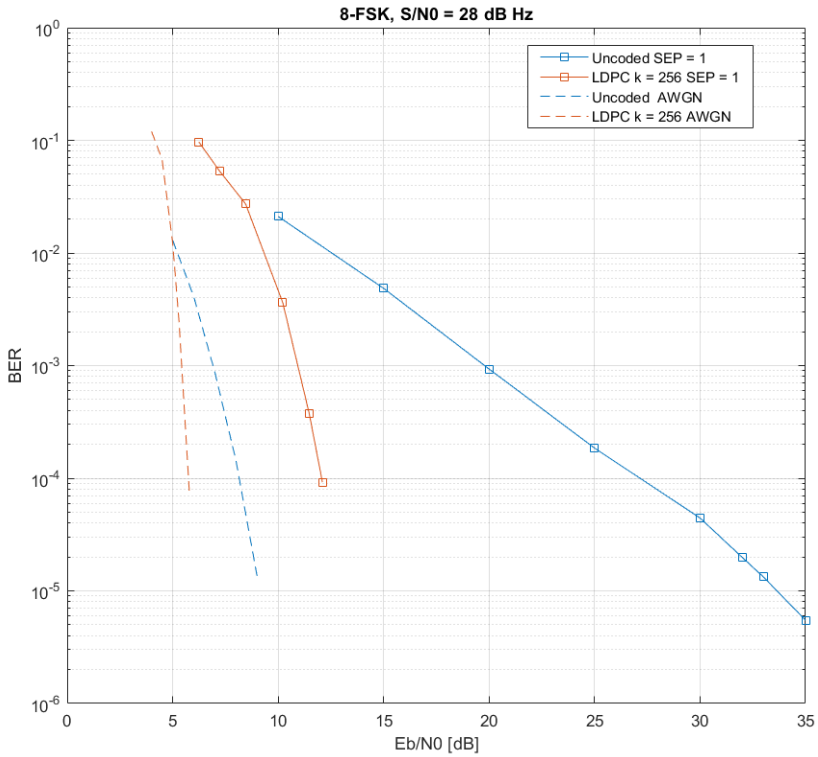

Figure 8-2 : BER (Bit Error Rate) vs Eb/N0 [dB] for the non-coherent 8-FSK modulation with an LDPC k = 256 and Uncoded case, at SEP = 1° and AWGN.

Obviously, the performances could be improved, since the LDPC coding schemes have been specifically designed and optimized assuming different coherent modulations (BPSK and QPSK) and the AWGN channel. There in principle is no reason why these coding schemes should perform close to the theoretical limits also with nonlinear modulations (such as M-FSK) and over channels with a nonergodic behaviour. But still, the LDPC codes are better (in terms of final performances) than uncoded. At very low SEP angles in particular, the degradation seen in the uncoded case is significantly larger than the one seen on LDPC (see Figure 8-2).

An ad-hoc code design may lead to new codes achieving higher coding gains. And moreover, also the channel diversity plays a fundamental role, since as soon as we approach the “non-ergodic zone”, the performances tend to degrade very quickly, so very probably any technique that can increase the channel diversity value (like interleaving) will bring a huge improvement in the performances.

8.3 Diversity

We consider two types of diversity, spatial where the same data stream is received at two spatially separated stations and frequency diversity. There are two different, but related, approaches to frequency diversity. The first is inter-band diversity (i.e. where the two, or more data streams are on widely separated carriers, e.g. X-band and Ka-band), while the second is in-band diversity (i.e. where the two, or more, data streams are on carriers separated in frequency but within the same band (e.g. X-band). For diversity systems to work, a key consideration is whether the different data streams are sufficiently decorrelated such that they can be considered independent. This is discussed for the case of signals during solar conjunctions in the following sections.

8.3.1 Spatial

Spatial diversity would allow signals to be transmitted and received from two separate locations on the earth, resulting in a diversity gain due to fades happening at different times on each path. There are two important considerations: firstly, what is the separation of the earth stations necessary to achieve significant decorrelation between the two signals and secondly, assuming a good decorrelation is achieved, how much can the error rate be improved.

As an initial approach to establishing the likely separation of stations on the earth where sufficient decorrelation of the signals will occur we have adopted a simple geometrical model. In Figure 8-3, rays joining the probe (P) to two stations on earth (A and B) is shown. Assuming the angle APB is small (which it will be), then PC is the probe-sun distance and PA is the earth-probe distance. AB is the distance between ground stations on the earth. The rays PA and PB have perihelia at C and D respectively, so CD is the distance which, when compared to the coherence length of variations in the coronal density, will determine whether the fading on the two signals is correlated.

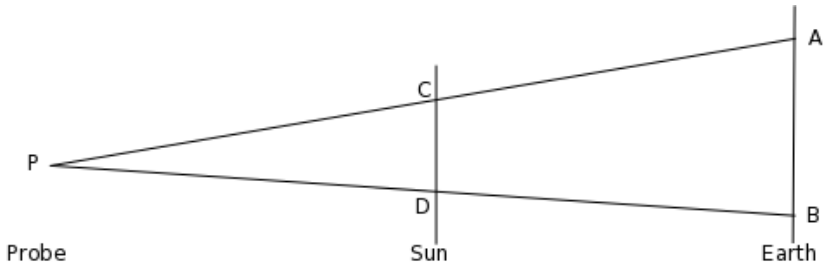

Figure 8-3 : Schematic of the probe (P) transmitting to two earth stations A and B.

Figure 8-4 shows the separation of ground-stations (AB) required to achieve the distance, *d* (=CD) between the two rays at their closest approach to the sun. It is seen that more distant probes will require less separation between ground-stations to achieve the same decorrelation between signals. In reality, the energy is not a pencil-beam, but is spread out over at least the first Fresnel zone, which is about 70 km in radius for X-band. While nothing confines the rays to just the Fresnel zone, it is true that the maximum of their power will lie within it. Therefore, taking each path as a beam of zero width is an approximation.

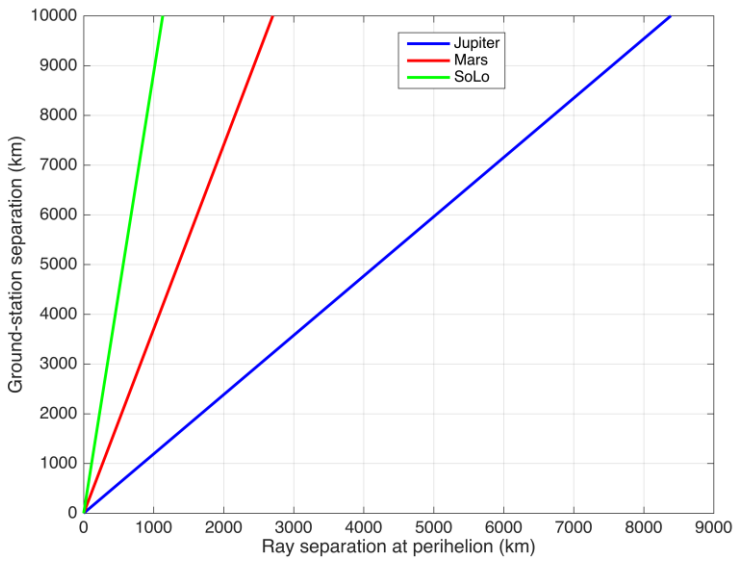

Figure 8-4 : Relation between the separation of ground-stations and separation at perihelion.

[RD. 2] state that correlations do not occur for distances greater than 50 km for X-band and 27 km for Ka-band, making spatial diversity possible at separations suitable for implementation. While this provides an answer, no explanation or

reference for these values are given by the authors. Therefore, we would recommend experimental tests before implementation is considered. A few practical suggestions, of varying difficulty follow.

- If two probes were able to transmit simultaneously, (say both orbiting Mars) and if they could be set to slightly different frequencies, then they could be received and compared to give the diversity gain directly. This may also be possible using two close radio stars, but the problem would then be to know what each signal was individually.

- An even more direct result would obviously be possible if two DSN receivers (*e.g.* one in Argentina and one in California) could receive the same signal.

- An upper limit on the spatial diversity gain could be attained by assuming complete independence between two signal paths and calculating the bit error rate compared to a single path. Errors are likely to occur during fades and with two ground stations there are four possible outcomes for each symbol, no fade on either signal, a fade on both signals, and a fade on one or other signal. This is expected to give a BER which is the product of the two individual BER values, as in the discussion on inter-band frequency diversity in 8.3.2.

From the above it appears that it is not clear whether spatial diversity will offer an improvement. On the one hand, a simple model (and values taken from the literature) would offer the required decorrelation over distances achievable on the surface of the earth, while a more complex approach suggests that it is reasonably unlikely that spatial diversity, even employing DSN ground-stations a few thousand km apart will offer much signal performance. However, in the latter case, further analysis of the data in the literature is necessary to be certain. Although there is plenty of data available, none of it seems to address diversity gain *per se*. Therefore, a more thorough understanding of the mathematical relations between diversity gain and, for example, phase PSD is required. Furthermore, the assumptions made above need to be tested more thoroughly.

8.3.2 Inter band Frequency diversity

During the MEX2013 solar conjunction event, observations of the open-loop carrier were made for X/X and X/S signals were made over a range of SEP. We have cross correlated the X-band and S-band signal amplitudes (after linearly detrending and applying a hamming window to reduce edge effects). Examples where 1000 s of observations have been correlated are presented Figure 8-5. The correlation between X-band and S-band signal amplitudes is close to zero (i.e. the amplitudes are uncorrelated) for all lags and for both values of SEP.

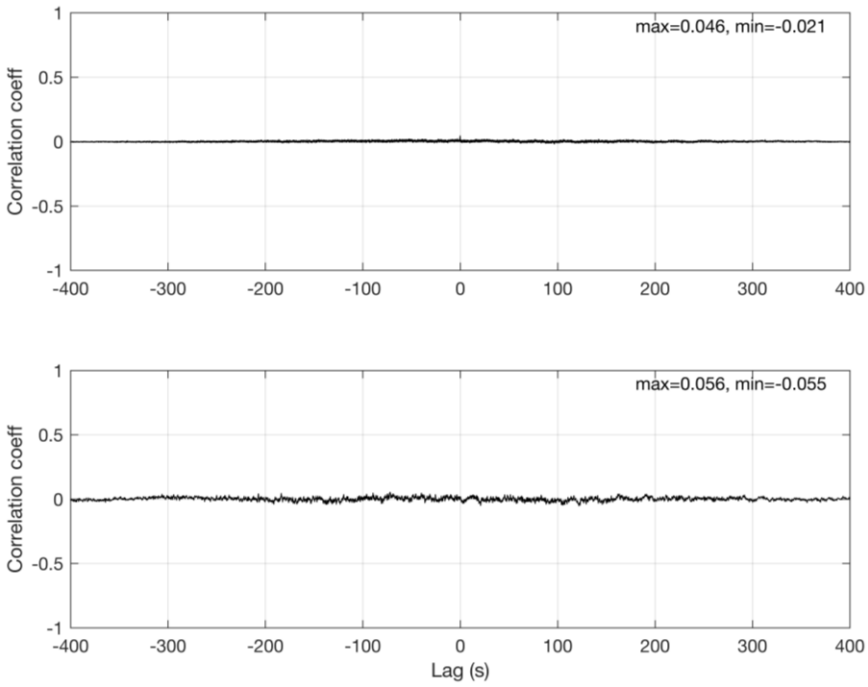

Figure 8-5 : Correlation coefficient for cross correlation between 1000 s of X-band and S-band amplitude for (top) SEP=9.8° and (bottom) SEP=2.1°.

Other two important considerations, taking aìinto account smaller intervals (1, 10, and 50 s) of the data were cross-correlated and the peak, positive, correlation found in each case, are :

- Firstly, that the correlation between the S- and X-band signals increases as the length of the interval of data being correlated decreases (although even at 1 s intervals, the correlation is not significant).
- Secondly, there is no systematic change in correlation with time, i.e. there are no periods where the signals are consistently more or less correlated than the mean level.

Having established that S-band and X-band signals are largely uncorrelated at a range of time-scales, it is likely that the same is true for Ka-band signals. So, it looks likely that inter band diversity will be possible during solar conjunctions. However, it is also important to consider the likely gains that could be made by employing inter band diversity. For example, assuming that transmitting simultaneously on two bands does not affect the power budget of either band (e.g. that the transmit power available for Ka-band is the same whether X-band is used or not) there are several regimes of operation:

1) Neither signal is significantly affected by the solar plasma (i.e. when SEP is high). In this case, there is nothing to be gained by transmitting the same data on both bands and diversity is not useful.

2) Both signals are affected by the solar plasma with the effects stronger on one signal than the other. For inter-band frequency diversity, this will always be the case with the lower frequency signal more affected than the higher frequency one. In this case, the data sent at the lower carrier frequency will experience more bit errors than those at the higher frequency. Therefore, operating on both frequencies with a diversity scheme will only tend to improve the performance when there is a bit error in the data on the higher frequency carrier but no error on the lower frequency carrier. For the case where the combining the streams in the diversity system is always able to find the correctly transmitted bit, if one exists, and the occurrence of errors on the two streams are independent, then the BER of the diversity system, P_D is given by

$$P_D = P_1 \cdot P_2 \qquad 8\text{-}1$$

where P_1 and P_2 are the probability of a bit error in data streams 1 and 2, respectively. For example, if the BER for one stream is 10^{-3} and is 10^{-2} for the other, then P_D=10^{-5}. It is very important to note that P_D represents the best possible performance that a diversity system would be capable of. For example, the improvement would be less where the system is not able to reliably determine when there is an error in one stream or the other (which would be the case when the BER is high) or where the errors in the streams are not independent. As demonstrated above, for inter-band frequency diversity, since the amplitude fading is not well correlated, then the second of these two conditions should be met, i.e. the errors will occur independently.

8.3.3 In-band frequency diversity

In common with the other diversity methods discussed here, how well in-band diversity will work depends on whether the occurrence of errors on the two (or more) data streams are independent. This, in turn, depends to a large extent on whether the amplitude fading is uncorrelated. There are no reported measurements of the correlation of amplitude fading resulting from propagation through the solar corona for signals across relatively narrow frequency ranges (e.g. a few MHz) and therefore no assessment of the potential efficacy of in-band frequency diversity can currently be made.

9 Final Remarks and Recommendations

9.1 Improvement of current Architecture and Methods

The end-to-end simulator developed as part of the project has been used to validate the results for a variety of different contingency scenarios. In most of the cases, i.e. the Test Scenarios provided, the symbol rate can be improved and the PLL bandwidth optimized compared to the values provided by ESA. However, two important things that should be considered, are:

- The optimum PLL bandwidth represents that calculated based on a conservative channel model (i.e. 90% of passes in MEX 2013 were better than this). Underestimating the PLL BW in the case where increasing solar plasma effects are present then increases the optimum PLL BW which has the potential for seriously impacting on the operation of the PLL is the chosen PLL BW is below this.
- Where an improved symbol rate is quoted this is the maximum value that still meets the ESA BER/FER requirement and therefore using data rates close to this maximum would not be robust against changes in the solar plasma conditions.

9.2 PLL performance at small SEP

At very low SEP angles, the increased level of amplitude fading means that phase jumps occur and there is an increase, for the duration of a fade, in the thermal phase noise.

The two parameters that have a large impact on the PLL performance are its bandwidth and the available CN0. Using different combinations of these two parameters and comparing the phase variance with a threshold value, i.e. 0.1 rad^2, the probability, $P_{critical}$ that a PLL would be unlikely to track the phase were obtained.

From this study, it is clear that at X-band, using coherent modulation too much below SEP=2° would be problematic unless very high values of CN0 are available (CN0>40 dB Hz may be available and this would allow the PLL to operate down to Sep~1.5° for X-band). Even if large CN0 would be available, the presence of phase slips, caused by the deep fading (e.g. ~40 dB for X-band at SEP=1°), are likely to remain a problem. For Ka-band, the intensity of amplitude fading

is lower and therefore the PLL tracking is sufficiently robust, thus coherent modulation methods could be used down to SEP~1° and possibly a littler lower than this.

9.3 Recommended coding scheme for coherent modulation

For the TC case the use of the two short LDPC codes (64/128 and 256/512) is recommended since they have better performance than the standard BCH 57/63;

For the TM case instead the choice is between the Turbo code and the LDPC. Comparing the codes with the same code rate, i.e. 1/2, the Turbo 8920 has better performances but exhibits a higher error floor. Taking this into consideration the LDPC k = 4096 appears as the most reliable. Moreover, longer LDPC, i.e. k = 16384, have not been simulated and are expected to provide even better results, since they will be even more "ergodic".

Instead, going to lower code rates (1/4 and 1/6), the Turbo code, provided that the PLL_{SNR} available is high enough, seems to be the recommended one. In particular, lower code rates have the advantage that at the same Eb/N0 the info rate is higher, but also the transmission time of a frame is higher. However, during the 2017 CCSDS Fall 2017 Meeting, a presentation by NASA/JPL reported about CCSDS turbo codes used within the STEREO mission. During the mission, contact with one of the spacecrafts, "STEREO-B", was lost prior to sun occultation (in October 2014) and was regained in August 2016. However, after contact was regained, the spacecraft was tumbling with no attitude control , which yielded an SNR characterized by deep fades.

After contact was regained, on August 27th, 2016, STEREO-B was using the CCSDS turbo code with information block length k=3568 and code rate R=1/6. Information bit rate was 11.6 bps, corresponding to a transmission time of 307.5 s per turbo codeword. As previously mentioned, due to absence of attitude control, the SNR was affected by deep fades. In particular, the channel exhibited a typical block fading behavior, with an alternation of "good channel state" (relatively large SNR) and "poor channel state" (deep fades). The channel diversity (number of different fading levels per codeword) was in the order of 5 to 6. A similar situation was observed on September 6th, 2016, when the information bit rate was 35 bps, with a codeword transmission time equal to 210 s. In this latter case the channel diversity was as low as 3. In both cases, the channel exhibited a typical non-ergodic behavior over the single codeword and turbo decoding turned out to be extremely challenging, with poor FER / BER. In NASA presentation it is explicitly remarked that this should not be surprising as CCSDS turbo codes where designed for an (ergodic) AWGN channel, not for a fading channel with correlated fading. This statement is in agreement with the conclusions of the HELIOS study.

For what concerns the channel diversity, in the uplink case it makes sense to use techniques that are able to increase L (like an interleaver), while for the TM case only for the shortest LDPC code, i.e. k=1024 is this needed, for the other codes the channel diversity is already high enough. This, as said before, remembering that in nominal cases the S/N0 value can be higher and so even the other codes could fall in the non-ergodic region, since the available symbol rate will be higher as well.

Another way to obtain better performance is represented by using the so-called "channel state information". In fact, over the solar plasma, the generic soft values observed by the channel decoder can be modelled as $y = (\alpha)\, x + n$, where $x \in \{-1,+1\}$ is the generic BPSK constellation symbol (real), n is a circularly-symmetric complex Gaussian random variable with zero mean and variance $N_0/2$ per dimension, i.e., $n = n_p + j\, n_q$ where n_p and n_q are both real, Gaussian, with zero mean and variance $N_0/2$; moreover n_p and n_q are statistically independent, α is a multiplicative complex coefficient due to solar plasma, y is the complex observable. The input to the belief propagation LDPC decoder (taken here as an example) depends on the availability of channel state information (CSI). Over fading channels, the demodulator typically estimates α (which is a random process

subject to random changes over the time): the best case is the one of ideal CSI information available at the receiver (α perfectly known for each y), while the worst one is unavailability of any CSI. In between, we have imperfect CSI. How to feed the LDPC decoder depends on CSI availability. Obviously the implementation of an algorithm to be used as a channel estimator of α, will increase the performance, since it will provide more accurate values of the LLR (log-likelihood ratio).

9.4 FSK

The use of modulation schemes different from BPSK, like FSK, is justified only when coherent demodulation cannot be used. In such cases, non-coherent demodulation schemes are recommended since this avoids the use of a PLL that, in these conditions, is significantly affected by the scintillation noise. The simulations demonstrated that having a reliable link at SEP=1° with an M-FSK modulation (in particular the most promising case is M = 8, since it provides the best "gain"[6] with respect to lower modulation order) is possible, even if this would mean to have lower info rates with respect to coherent modulation.

Finally, it was clear that the codes that are used for coherent modulation, like the LDPC, are not very well suited for non-coherent modulation. So, this suggests that ad hoc codes should be implemented for the non-coherent case.

9.5 Diversity

Two options have been discussed: spatial and inter band frequency diversity.

From our work, it is unclear whether spatial diversity will lead to significant improvements. A simple model together with values of the solar corona plasma scale-size suggests that antenna separations of 100 km or so will provide the necessary decorrelation. However, a more complex model suggests that the even antenna separations of a few thousand km are unlikely to offer much diversity gain. In our view, experimental tests or analysis of the data in the literature (if any become available) are necessary to be certain.

Inter-band frequency diversity seems like a feasible solution since the observed S-band and X-band signals are largely uncorrelated, and, by inference, this is likely to be true for X-band and Ka-band. The maximum possible performance gains that could be made by employing inter band diversity have been presented.

[6] The 16-FSK does not guarantee a gain in performance with respect to 8-FSK, that is enough to justify its use.

9.6 Development needs

In the next few tables we provide development suggestions, as provided by Thales based on a previous analysis we performed on the complexity analysis of the new CCSDSLDPC codes for TC/TM, and the use of non-coherent FSK.

Item/Function	Outline of Implementation	Implementation Steps	Timeline	Other considerations
LDPC Decoding. The LDPC decoder is implemented following output from previous ESA study "*Next Generation Uplink Coding Techniques*" (NEXCODE).	A LDPC decoder breadboard will be validated together with DST Engineering Model in the frame of the on-going ESA study "*Flexible and Autonomous TT&C Transponders for Multi Mission Applications*" (FAT). Then the relevant VHDL IP has to be synthesized towards space-qualified FPGA (baseline: RTG4)	Breadboard validation Synthesis towards RTG4 Validation at DST-level using RTG4 prototype	4Q/2017 To+2 To+6	It includes electrical redesign of the Digital, updating of the manufacturing documentation and delta-analysis (WCA, PSA, etc). DEIMOS cost for LDPC IP to be assessed.

Item/Function	Outline of Implementation	Implementation Steps	Timeline	Other considerations
Frequency-diversity. The same signal in PM/BPSK/NRZ or PM/SP-L modulation format is transmitted in X-Band with a frequency separation in the range from 8 to 10 MHz.	It requires a modification of the X-Band Transmitter module in the relevant Baseband section that needs to combine the two down-link signals at the input of the frequency conversion stages	The hardware modification is straightforward and does not require a specific validation phase through breadboard. It can be directly pursued in the frame of a flight Program.	Not applicable	It includes electrical redesign of the X-Band Transmitter Module, updating of the manufacturing documentation and delta-analysis (WCA, PSA, etc).

M-FSK TC Demodulator. The DST supports M-FSK in addition to the standard telecommand modulation formats. The operative signalling scheme has to be selected by a dedicated 1553 command.	A space-qualified FPGA (baseline: RTG4) will integrate the relevant signal processing blocks. Such FPGA may also include down-link GMSK/M-FSK/DPSK processing.	Algorithm definition Specification VHDL Design & Simulation Breadboard test	To+2 To+4 To+8 To+12	It includes electrical redesign of the Digital, updating of the manufacturing documentation and delta-analysis (WCA, PSA, etc).

Item/Function	Outline of Implementation	Implementation Steps	Timeline	Non-recurring ROM Cost for the 1st Program
M-FSK TM Modulator. The DST supports M-FSK in addition to other telemetry modulation formats (residual carriers and suppressed carrier). The operative signalling scheme has to be selected by a dedicated 1553 command.	A space-qualified FPGA (baseline: RTG4) will integrate the relevant signal processing blocks proving to the X-Band Vector Modulator the in-phase and quadrature modulating streams according to the selected modulation format. Such FPGA may also include M-FSK TC Demodulator.	Algorithm definition Specification VHDL Design & Simulation Breadboard test	To+1 To+3 To+6 To+9	It includes electrical redesign of the Digital, updating of the manufacturing documentation and delta-analysis (WCA, PSA, etc).